

DESIGN OF THE SUPERCONDUCTING RFQ1 CAVITY FOR THE PIAVE LINAC

T. Shirai ¹, G. Bisoffi ² and V. Andreev ²

¹ Nuclear Science Research Facility, ICR, Kyoto University, Kyoto, Japan

² INFN - Laboratori Nazionali di Legnaro, Padova, Italy

1. INTRODUCTION

In the new injector PIAVE (Positive Ion Accelerator for Very-low Energy), two superconducting RFQs will be used. Table 1 shows the basic parameters of SRFQ1 and SRFQ2 [1]. The cavity design of SRFQ2 was determined and the model construction is proceeding [2]. The cavity design of SRFQ1 is based on that of SRFQ2. It has a 4-rod structure with a scheme of alternate stems. It has a good mode separation between the quadrupole and the dipole modes. Due to the alternate stems, the voltage is created between the end of the vane and the end wall. It can be used for the beam acceleration and it is very effective for the low energy beam. The components of the cavity will be made of 3 mm thick niobium (Nb) sheet. They will be assembled by the electron beam welding (EBW).

The major difference between the two cavities is the vane length. The vane of SRFQ1 is about twice as long as that of SRFQ2. The EBW is difficult due to the length because we have to rotate the vane and the tank in the vacuum chamber for the EBW. The EBW of SRFQ1 requires the vacuum chamber which is larger than 3 m. But such a large machine is not available. We propose to divide the vane and the tank into two parts. Figure 1 shows the schematic view of the vanes and the stems of SRFQ1. The cutting point is at the center between the stems to minimize the field disturbance. Finally the two tanks are welded by the EBW into one cavity.

Table1 Basic parameters of two SRFQs*

	SRFQ1	SRFQ2
Resonant Frequency (MHz)	80.0	80.0
Vane length (mm)	1378	746.1
Output Energy (keV/u)	341.7	578.3
Vane voltage (kV)	148	280
Ave. aperture (mm)	8	15.3
Modulation	1.2 - 3	3

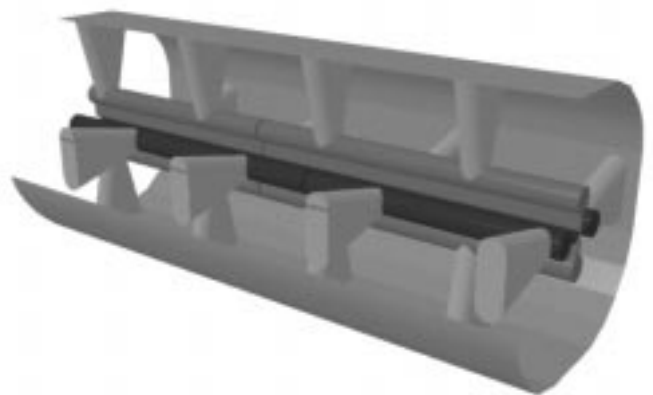


Figure 1 Schematic view of SRFQ1

* The mass over charge ratio 8.5 ($^{+28}\text{U}^{238}$) is assumed.

2. GEOMETRY OF SRFQ1

The dimension of SRFQ1 is shown in the figure 2. We adopt the same hollow cylinders and the stems as those of SRFQ2. They are designed based on the mechanical vibration analysis. We can also make the best use the experiences in construction and welding for SRFQ2. The position of the hollow cylinder is optimized by M.A.F.I.A. electrostatic solver (S-3). We choose the distance of 7 cm because the vane capacitance difference in the case of 7 cm and 7.5 cm is less than 1 % of the total capacitance.

The number of the stems is four: thus each split vane has two stems for the mechanical stability. The transverse electric field distribution along the axis is simulated by M.A.F.I.A. eigenvalue solver (E-3). No modulation is assumed in the input geometry data for M.A.F.I.A. Figure 3 (a) shows the result when the distances between each stem are equal. The field bump is 1.3 %. The field

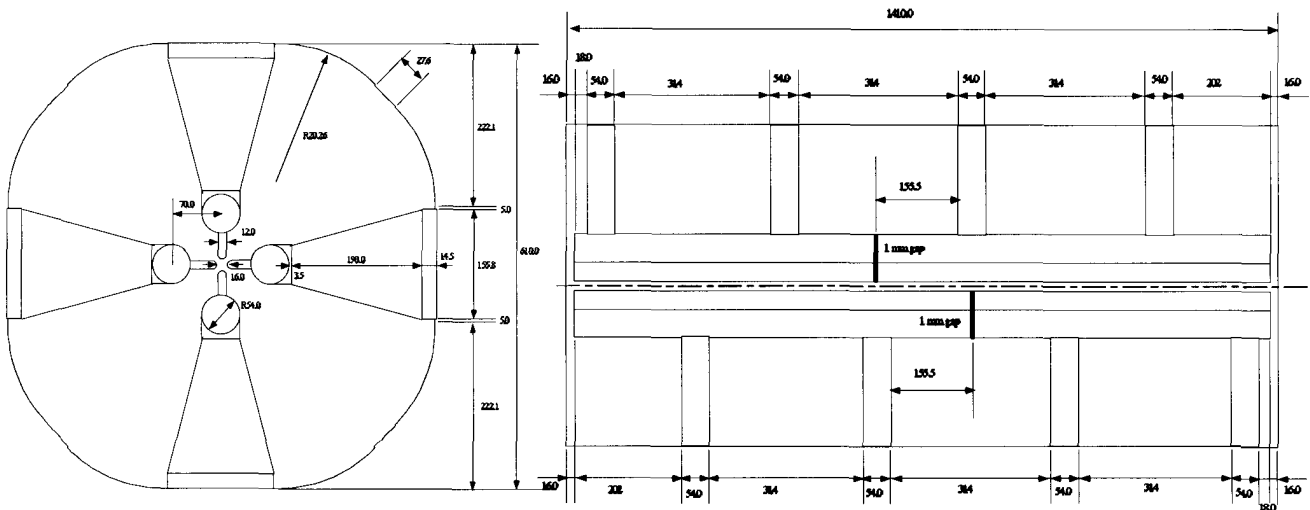


Figure 2 Dimension of SRFQ1 cavity

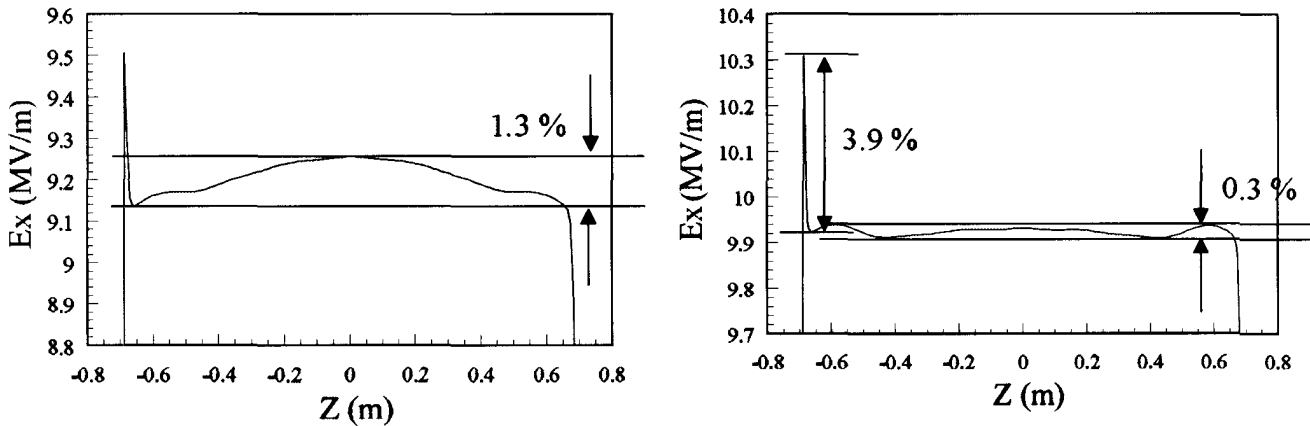


Figure 3 Close view of the bump of the transverse electric field. It is evaluated at X=4.2 mm along the beam axis. (a): Before field compensation. (b): After field compensation, the distance between the center of the end stem and the vane end is 18 mm.

distribution is disturbed by an effect of the end cell. To compensate the field bump, the end stem position is shifted toward the cavity center while the distances between stems are kept constant. The inductance of the end region increases relatively by the shift. The result is shown in Fig. 3 (b). The field bump becomes 0.3 %, where the distance between the center of the end stem and the vane end is 18 mm long. A field spike of 3.9 % is found at the end of the vane in Fig. 3(b). It is an effect of the end wall. It is an inevitable feature in this structure and the effect on the beam dynamics was evaluated by the particle simulation.

3. EFFECT OF THE VANE GAP

The two split tanks will be welded eventually to construct the cavity. But the vanes tip and the hollow cylinder inside the tanks are not united and small gaps exist between them (shown in figure 4) because the welding of the vane tip is technically impossible. With the effect of the vane gaps, the lowest quadrupole mode is split into three ones. Figure 4 shows the some mode frequencies with various gap width. The quadrupole mode 3 is an operation one. In the other modes, the direction of the current flow changes at the gap positions and the resonant frequency has a strong dependence on the gap width. We adopt 1 mm gap width because the mode separation is not sufficient with a wider gap and the tolerance of the construction and the alignment error are too tight in the smaller gap.

Another effect from the gap is a perturbation on the electric field around the gap. It is simulated by M.A.F.I.A. S-3. Figure 5 shows the longitudinal distribution of the transverse electric field at X=4 mm. The field dip appears at the gap center but the dip is only 0.2 % with the 1 mm gap.

The gap position is optimized by M.A.F.I.A. E-3. It should be placed where the longitudinal current on the vane is zero, otherwise a voltage jump is created by the gap capacitance. Equivalently, the transverse magnetic field on the vane should be also zero at the gap. The magnetic field can be

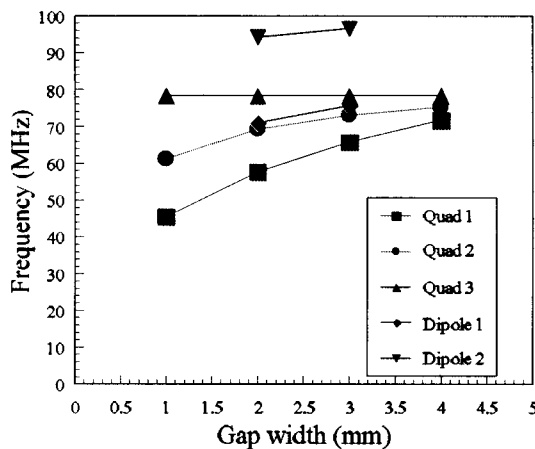


Figure 4 Some mode frequencies with various gap width. Three quadrupole and two dipole modes are calculated by M.A.F.I.A. E-3.

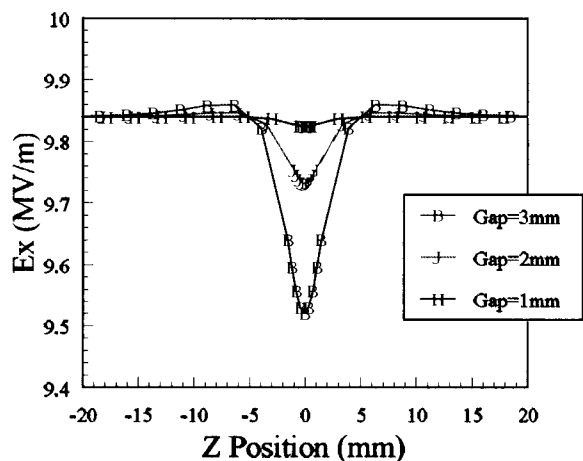


Figure 5 Transverse electric field distribution around the gap. The field is evaluated at X=4 mm

Table 2 M.A.F.I.A. simulation results of SRFQ1

Resonant Frequency (MHz)	79.9
Gap voltage (kV)	148.0
Stored energy (J)	2.1
Capacitance (pF/m)	142
Max. electric field (MV/m)	25.5
Max. magnetic field (Gauss)	249
Shunt impedance ($M\Omega/m$) (Cu)	0.200
Power Loss (kW) (Cu)	79.6
Q value (Cu)	13200

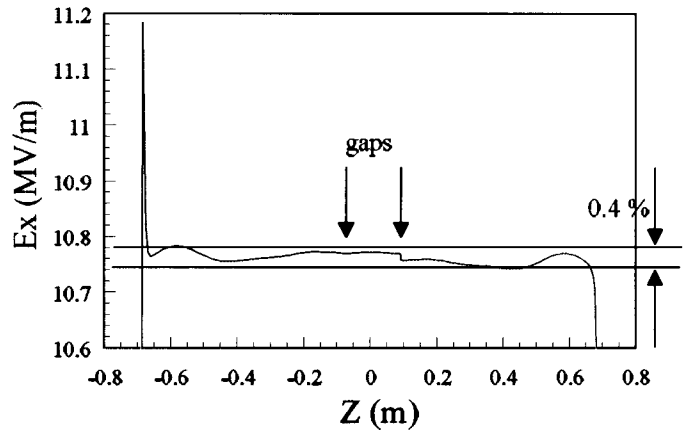


Figure 6 Close view of the transverse field bump with 1 mm gaps. The field is evaluated at $X=4.2$ mm

calculated by M.A.F.I.A. E-3 and the gap position is determined to be 9.15 cm from the center of the cavity. Figure 6 shows a simulation result of the field distribution with 1 mm gaps. The field bump is 0.4 % and the difference from the result of Fig. 3(b) is only 0.1 %.

Table 2 shows the M.A.F.I.A. E-3 simulation results on SRFQ1. The maximum magnetic field of 249 Gauss is lower than the critical field of Nb at 4K. The maximum electric field of 25.5 MV/m is also lower than that of the typical quarter-wave resonators at INFN-LNL. The stored energy is 2.1 J, which is smaller than that of SRFQ2 and acceptable from the view point of RF control.

4. ACKNOWLEDGMENTS

The authors would like to thank to A. Pisent, M. Comunian and A. Lombardi who had many discussions with us about the cavity structure. We also thank to A. Noda and Y. Iwashita for their advises.

REFERENCES

- [1] A. Pisent et al., "Complete Simulation of the Heavy Ion Linac PIAVE", Proc. of the 1997 Particle Accelerator Conference, Vancouver
- [2] G. Bisoffi et al., "Prototype of a Superconducting RFQ for a Heavy Ion Injector Linac", Proc. of the 1997 Particle Accelerator Conference, Vancouver